

Molecular Frustration of Chemically Linked Rod-Disc Liquid Crystal under an Electric Field

Jun Ho Jung,[†] So-Eun Kim,[†] Eun Kyoung Song,[†] Kyung Su Ha,[†] Namil Kim,[‡]
Yan Cao,[‡] Chi-Chun Tsai,[‡] Stephen Z. D. Cheng,[‡] Seung Hee Lee,^{*,†} and
Kwang-Un Jeong^{*,†}

[†]Polymer BIN Fusion Research Center, Department of Polymer-Nano Science and Technology, and
Department of BIN Fusion Technology, Chonbuk National University Jeonju, Jeonbuk 561-756, Korea, and
[‡]College of Polymer Science and Polymer Engineering, The University of Akron, Akron, Ohio 44325-3909

Received May 19, 2010. Revised Manuscript Received July 8, 2010

Molecular orientation of a chemically linked rod-disk (cyanobiphenyl-triphenyl) liquid crystalline (LC) molecule (RD12, where 12 is a number of carbon atoms in each alkyl chain linkage between the rod and the disk mesogens) in an antiparallel rubbed LC cell was investigated under vertically applied alternative current (AC) electric fields. Upon varying vertical AC electric fields from the initial state (0 V) to a fixed voltage ranging between 2.5 and 5.0 V, it was found that RD12 responded to the electric field with two-steps. The rod mesogen having a higher dipole interaction first aligned parallel to the electric field, while the disk mesogen behaved like an anchor of RD12. After the frustration and stabilization of rod mesogens, the in-plane axis of disk mesogen also aligned parallel to the electric field. Based on our experimental results, it was concluded that the peculiar molecular frustrations of RD12 under the vertical AC electric field occurred in a consequence of the competition among rods attached to both sides of the disk molecule. Furthermore, because molecular orientation of RD12 exhibiting a large birefringence is controlled by an electric field, RD12 can be used as a tunable optical switching material in the electro-optical devices.

Introduction

To improve electro-optic characteristics of liquid crystal displays (LCDs), design, synthesis, and characterization of complex LC molecules have been explored since the first discovery of LC materials in the 1880s.^{1–11} Thanks to these efforts, LCD is a ubiquitous and superior

display compared with others.^{12–20} Parallel to the practical applications of LCs, novel LC phases such as twist grain boundary phases,^{21–23} blue phases,^{24–26} achiral banana phases^{27–32} and biaxial nematic (N) LC phases^{33–36} have been obtained by introducing different chemical functions as well as by synthesizing novel geometry of LC molecules.

- *To whom the correspondence should be addressed. E-mail: lsh1@chonbuk.ac.kr (S.H.L.); kujeong@chonbuk.ac.kr (K.-U.J.).
- (1) Osipov, M. A. In *Handbook of Liquid Crystals*; Demus, D., Goodby, J., Gray, G. W., Spiess, H.-W., Vill, V., Eds.; Wiley-VCH: Weinheim, Germany, 1998; Vol. 1, Chapter 2.
 - (2) Kelker, H.; Knoll, P. M. *Liq. Cryst.* **1989**, *5*, 19.
 - (3) Lehmann, O. *Z. Phys. Chem.* **1888**, *9*, 421.
 - (4) Tammann, G. *Ann. Phys.* **1901**, *3*, 524.
 - (5) Demus, D.; Gloza, A.; Hartung, H.; Hauser, A.; Rapthel, I.; Wiegeleben, A. *Cryst. Res. Technol.* **1981**, *16*, 1445.
 - (6) Levelut, A.-M.; Donnio, B.; Bruce, D. W. *Liq. Cryst.* **1997**, *22*, 753.
 - (7) Chandrasekhar, S.; Sadashiva, B. K.; Suresh, K. A. *Pramana* **1977**, *9*, 471.
 - (8) Schadt, M.; Bucheker, R.; Mueller, K. *Liq. Cryst.* **1989**, *5*, 293.
 - (9) Kim, Y. C.; Lee, S. H.; West, J. L.; Gelerinter, E. *J. Appl. Phys.* **1995**, *77*, 1914.
 - (10) Lee, S. H.; Lee, S. L.; Kim, H. Y.; Eom, T. Y. *J. Korean Phys. Soc.* **1999**, *35*, 1111.
 - (11) Wang, P.; Moorefield, C. N.; Jeong, K. -U.; Hwang, S. -H.; Li, S.; Cheng, S. Z. D.; Newkome, G. R. *Adv. Mater.* **2008**, *20*, 1381.
 - (12) Schadt, M.; Helfrich, W. *Appl. Phys. Lett.* **1971**, *18*, 127.
 - (13) Mori, H.; Itoh, Y.; Nishiura, Y.; Nakamura, T.; Shinagawa, Y. *Jpn. J. Appl. Phys.* **1997**, *36*, 143.
 - (14) Petkovsek, R.; Copic, M.; Pirs, J. *J. Appl. Phys.* **2006**, *99*, 44103.
 - (15) Komitov, L.; Olsson, N.; Helgåe, B. *Appl. Phys. Lett.* **2006**, *89*, 121919.
 - (16) Kim, Y. T.; Hong, J. H.; Yoon, T. Y.; Lee, S. D. *Appl. Phys. Lett.* **2006**, *88*, 263501.
 - (17) Oh-e, M.; Kondo, K. *Appl. Phys. Lett.* **1995**, *67*, 3895.
 - (18) Lee, S. H.; Lee, S. L.; Kim, H. Y. *Appl. Phys. Lett.* **1998**, *73*, 2881.

- (19) Hong, S. H.; Jeong, Y. H.; Kim, H. Y.; Cho, H. M.; Lee, W. G.; Lee, S. H. *J. Appl. Phys.* **2000**, *87*, 8259.
- (20) Park, J. W.; Ahn, Y. J.; Jung, J. H.; Lee, S. H.; Lu, R.; Kim, H. Y.; Wu, S. -T. *Appl. Phys. Lett.* **2008**, *93*, 081103.
- (21) Leadbetter, A. J.; Gaughan, J. P.; Kelly, B.; Gray, G. W.; Goodby, J. *J. Phys. Colloq. C3* **1979**, *40*, 178.
- (22) de Gennes, P. G. *Solid. State Commun.* **1972**, *10*, 753.
- (23) Renn, S. R.; Lubensky, T. C. *Phys. Rev. A* **1988**, *38*, 2132.
- (24) Crooker, P. P. *Liq. Cryst.* **1989**, *5*, 751.
- (25) Coates, D.; Gray, G. W. *Phys. Lett. A* **1973**, *45*, 115.
- (26) Gerber, P. R. *Mol. Cryst. Liq. Cryst.* **1985**, *116*, 197.
- (27) Niori, T.; Sekine, T.; Watanabe, J.; Furukawa, T.; Takezoe, H. *J. Mater. Chem.* **1996**, *6*, 1231.
- (28) Dantigraber, G.; Shen, D.; Diele, S.; Tschierske, C. *Chem. Mater.* **2002**, *14*, 1149.
- (29) Reddy, R. A.; Raghunathan, V. A.; Sadashiva, B. K. *Chem. Mater.* **2005**, *17*, 274.
- (30) Jeong, K. -U.; Yang, D. -K.; Graham, M. J.; Tu, Y.; Kuo, S. -W.; Knapp, B. S.; Harris, F. W.; Cheng, S. Z. D. *Adv. Mater.* **2006**, *18*, 3229.
- (31) Folcia, C. L.; Alonso, I.; Ortega, J.; Etchebarria, J.; Pintre, I.; Ros, M. B. *Chem. Mater.* **2006**, *18*, 4617.
- (32) Yoshioka, T.; Ogata, T.; Nonaka, T.; Moritsugu, M.; Kim, S. -N.; Kurihara, S. *Adv. Mater.* **2005**, *17*, 1226.
- (33) Yu, L. J.; Saupé, A. *Phys. Rev. Lett.* **1980**, *45*, 1000.
- (34) Brand, H.; Pleiner, H. *Phys. Rev. A* **1981**, *24*, 2777.
- (35) Liu, M. *Phys. Rev. A* **1981**, *24*, 2720.
- (36) Francescangeli, O.; Stanic, V.; Torgova, S. I.; Strigazzi, A.; Scaramuzza, N.; Ferrero, C.; Dolbnya, I. P.; Weiss, T. M.; Berardi, R.; Muccioli, L.; Orlando, S.; Zannoni, C. *Adv. Funct. Mater.* **2009**, *19*, 2592.

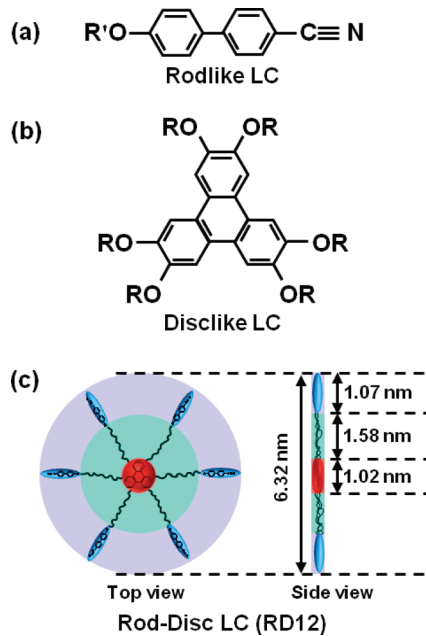


Figure 1. Chemical structures of (a) cyanobiphenyl calamitic LC, (b) triphenyl discotic LC, and (c) RD12.⁴⁹ Calculated geometric dimensions of RD12 were schematically illustrated with top and side views in panel c.

Among them, intensive researches on chemically connected rod-disk LC molecules have been focused on to fill the gap between discotic (disklike) and calamitic (rodlike) LCs and to examine the existence of biaxial N phase.^{37–42} Unlike common rodlike LCs that exhibit uniaxial positive birefringence with the optic axis parallel to the molecular long axis,

- (37) Houbenov, N.; Nykänen, A.; Iatrou, H.; Hadjichristidis, N.; Ruokolainen, J.; Faul, C. F. J.; Ikkala, O. *Adv. Funct. Mater.* **2008**, *18*, 2041.
- (38) Shimizu, Y.; Kurobe, A.; Monobe, H.; Terasawa, N.; Kiyohara, K.; Uchida, K. *Chem. Commun.* **2003**, 1676.
- (39) Date, R. W.; Bruce, D. W. *J. Am. Chem. Soc.* **2003**, *125*, 9012.
- (40) Ge, J. J.; Hong, S. -C.; Tang, B. Y.; Li, C. Y.; Zhang, D.; Bai, F.; Mansdorf, B.; Harris, F. W.; Yang, D.; Shen, Y. -R.; Cheng, S. Z. D. *Adv. Funct. Mater.* **2003**, *13*, 718.
- (41) Kouwer, P. H. J.; Mehl, G. H. *Angew. Chem., Int. Ed.* **2003**, *42*, 6015.
- (42) Jeong, K. -U.; Jin, S.; Ge, J. J.; Knapp, B. S.; Graham, M. J.; Ruan, J.; Guo, M.; Xiong, H.; Harris, F. W.; Cheng, S. Z. D. *Chem. Mater.* **2005**, *17*, 2852.
- (43) Jeong, K. -U.; Knapp, B. S.; Ge, J. J.; Jin, S.; Graham, M. J.; Harris, F. W.; Cheng, S. Z. D. *Chem. Mater.* **2006**, *18*, 680.
- (44) Jeong, K. -U.; Jing, A. J.; Mansdorf, B.; Graham, M. J.; Tu, Y.; Harris, F. W.; Cheng, S. Z. D. *Chin. J. Polym. Sci.* **2007**, *25*, 57.
- (45) Xue, C.; Jin, S.; Weng, X.; Ge, J. J.; Shen, Z.; Shen, H.; Graham, M. J.; Jeong, K.-U.; Huang, H.; Zhang, D.; Guo, M.; Harris, F. W.; Cheng, S. Z. D.; Li, C. Y.; Zhu, L. *Chem. Mater.* **2004**, *16*, 1014.
- (46) Shen, H.; Jeong, K. -U.; Xiong, H.; Graham, M. J.; Leng, S.; Zheng, J. X.; Huang, H.; Guo, M.; Harris, F. W.; Cheng, S. Z. D. *Soft Matter* **2006**, *2*, 232.
- (47) Hwang, S. H.; Lim, Y. J.; Lee, M. -H.; Lee, S. H.; Lee, G. -D.; Kang, H.; Kim, K. J.; Choi, H. C. *Curr. Appl. Phys.* **2007**, *7*, 690.
- (48) Fletcher, I. D.; Luckhurst, G. R. *Liq. Cryst.* **1995**, *18*, 175.
- (49) Jeong, K. -U.; Jing, A. J.; Monsdorf, B.; Graham, M. J.; Harris, F. W.; Cheng, S. Z. D. *J. Phys. Chem. B* **2007**, *111*, 767.
- (50) Jeong, K. -U.; Jing, A. J.; Mansdorf, B.; Graham, M. J.; Yang, D. -K.; Harris, F. W.; Cheng, S. Z. D. *Chem. Mater.* **2007**, *19*, 2921.
- (51) Hwang, S. -H.; Park, S. -J.; Kim, H. Y.; Kuo, S. -W.; Lee, S. H.; Lee, M. -H.; Jeong, K. -U. *J. Phys. Chem. B* **2009**, *113*, 5843.
- (52) Park, S. -J.; Hwang, S. -H.; Kim, N.; Kuo, S. -W.; Kim, H. Y.; Park, S. -K.; Kim, Y. -J.; Nah, C.; Lee, J. H.; Jeong, K. -U. *J. Phys. Chem. B* **2009**, *113*, 13499.
- (53) Leng, S.; Chan, L. H.; Jing, J.; Hu, J.; Moustafa, R. M.; Van Horn, R. M.; Graham, M. J.; Sun, B.; Zhu, M.; Jeong, K. -U.; Kaafarani, B. R.; Zhang, W.; Harris, F. W.; Cheng, S. Z. D. *Soft Matter* **2010**, *6*, 100.

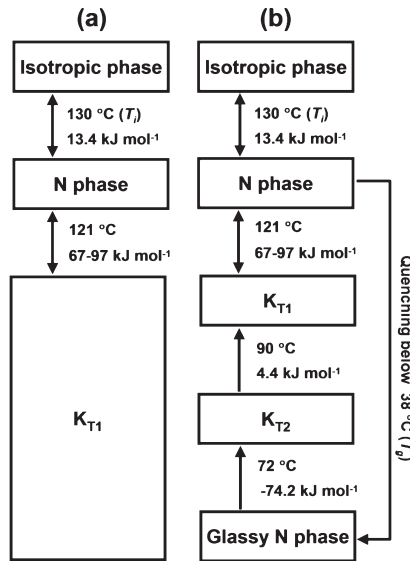


Figure 2. Phase transition diagrams of RD12⁴⁹ (a) during cooling and subsequent heating at 2.5 °C/min, and (b) during heating at 2.5 °C/min after quenching from the N phase below T_g .

disklike LCs possess intrinsically uniaxial negative birefringence with the optic axis perpendicular to the disk-plane.^{43–53} The competition between the excluded volumes of extremely different two mesogens in the chemically connected rod-disk LC molecules may result in a biaxial molecular orientation.

Recently, Cheng and his co-workers reported the characteristics of the rod-disk molecule (RD12), which was newly synthesized by the chemical combination of rodlike (R) and disklike (D) mesogens.^{49,50} The chemical structures and its geometric dimensions are illustrated in Figure 1. Through combined experimental results and careful analyses, it was realized that RD12 molecule can form three different ordered phases by decreasing temperature from isotropic (I) phase: N phase, stable K_{T1} crystalline phase, and metastable K_{T2} crystalline phase (Figure 2).⁴⁹ Furthermore, they demonstrated the existence of biaxial N phase under the direct current (DC) electric field, even though a macroscopically stable uniform biaxial domain was not obtained.⁵⁰ However, RD12 molecular orientations and transition behaviors under the alternative current (AC) electric fields with alignment layers have not been understood. Therefore, there are a few questions remaining. What are the RD12 molecular orientations and behaviors under various AC electric fields with a planar alignment layer? Molecular behaviors of RD12 under AC electric fields can be important not only for the scientific studies but also for the practical applications in LCDs. What is the birefringence of RD12 molecule? On the basis of the molecular geometry of RD12, RD12 can exhibit a large birefringence, which can be useful in thin optical compensation films. Furthermore, when birefringence of optical films made of RD12 can be controlled by magnetic and/or electric fields, tunable optical switches may be fabricated.

To answer these questions, we first fabricated an anti-parallel-rubbed electro-optic LC cell, which is one of the

typical LCD modes. By varying vertical AC electric fields, optical textures and normalized light transmittances were monitored with respect to time. On the basis of these experiments, it was obviously realized that RD12 molecules were oriented parallel to the electric field by two-step processes. Rod mesogens having a higher dipole interaction first aligned parallel to an electric field. However, rod mesogens on both sides of the discotic mesogen competed with each other to align parallel to the vertical electric field. This competition among the rod mesogens resulted in molecular frustration and abnormal transmittance changes. After the stabilization of rod mesogens, the in-plane axes of disk mesogens subsequently aligned parallel to an electric field. Based on systematic experiments and careful analyses, possible molecular orientations under the vertical AC electric fields were proposed. The suggested models of molecular arrangements at each condition were further supported by the observation of optical textures.

Equipment and Experiments

A rod-disk liquid crystalline (LC) molecule (RD12) was synthesized by four-step condensation reactions.⁴⁹ The chemical structure of RD12 molecule purified by chromatography on silica gel using chloroform/hexane (6/1) mixed solvent as an eluent was verified by thin-layer chromatography, MALDI-TOF mass spectrometry, elemental analysis, and proton nuclear magnetic resonance spectroscopy (¹H NMR).⁴⁹ The Cerius² (Version 4.6, Accelrys) simulation software with the COMPASS force field was applied to estimate the energy minimized geometry of RD12 in the isolated gas-phase and the results were schematically illustrated in Figure 1. The calculated diameter of the triphenyl discotic core was 1.02 nm and the length of each cyanobiphenyl rod was 1.07 nm. When the alkyl chains between six rods and one disk were assumed to be in the all-*trans* conformation, the diameter of RD12 molecular disk was calculated to be 6.32 nm, as shown in Figure 1.

In order to confirm the molecular orientation of RD12 molecule under the vertical electric field, the antiparallel-rubbed electro-optic LC cells were fabricated with planar alignment layer (Japan Synthetic Rubber, AL-16139, Japan) coated on indium tin oxide (ITO) glass substrates. This type of LC cell is called as electrically controlled birefringence (ECB) cell.^{54–56} Using a spin coater (Korea Spin Coater system, ECF-2, Korea), planar alignment layer was first coated on ITO glass substrates. The spinning rate was increased up to 2800 rpm and maintained for 70 s after the spin coating at 550 rpm for 20 s. The spin coated substrates were cured in a drying oven (JEIO TECH, NO-600M, Korea) with two-step processes. After being cured for 5 min at 80 °C, the spin-coated substrates were further cured for 1 h at 180 °C to secure the adhesion between ITO glass substrate and alignment layer. The thickness of cured planar alignment layers was controlled to be 100 nm. After rubbing process for the antiparallel alignment of RD12, two substrates were assembled into a sandwich LC cell by utilizing automatic press (Neo system, APD-01, Japan). In this assembling process, plastic ball spacers with a diameter of about 4.5 μm were purposely added between the substrates in order to maintain the uniform cell gap.

(54) Schiekel, M. F.; Fahrenschon, K. *Appl. Phys. Lett.* **1971**, *19*, 391.
 (55) Soref, R. A.; Rafuse, M. J. *J. Appl. Phys.* **1972**, *43*, 2029.
 (56) Ong, H. L. *Appl. Phys. Lett.* **1991**, *59*, 155.

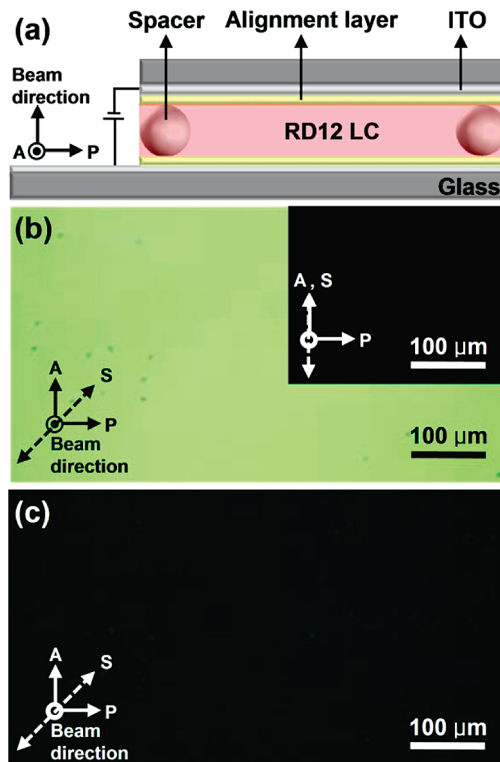


Figure 3. (a) Schematic illustration of the RD12-filled ECB cell. POM images with 45° deviation of the rubbed direction (S) from analyzer (A) and polarizer (P) in the N phase at different AC electric fields: (b) 0 and (c) 15 V. The inset POM image in b was obtained when S was aligned parallel to A.

Using a cell gap measurement (Sesim Photonics Technology, CGMS-100T, Korea), the cell gap was experimentally determined to be 4.43 μm. Using osmotic pressure, RD12 was injected into the fabricated LC cell at 122.7 °C, in which RD12 is in the N phase. Schematic structure of the fabricated RD12-filled ECB cell was illustrated in Figure 3. Polarizer (P) and analyzer (A) were arranged perpendicular to each other and the antiparallel rubbing direction (S) of substrate was set to be 45° with respect to P and A. The birefringence (Δn) of RD12 in N LC phase was estimated to be 0.172 by utilizing POM combined with Michel-Lévy birefringence chart.⁵⁷ The birefringence of RD12 was also confirmed by the measurement of retardation ($d\Delta n$) of RD12 in which thickness (d) was previously known (Sesim Photonics Technology, REMS-150, Korea). Pretilt angle (ϕ) of RD12 was also measured by an optic system (Sesim Photonics Technology, PAMS-100T, Korea).

Phase transitions of the RD12-filled ECB cell were investigated by texture observations using POM (Nikon, Eclipse E650 POL, Japan) equipped with a temperature controller (Linkam, TMS94, UK). The temperature and cooling/heating rate of this hot stage were calibrated in range of ± 0.5 °C and ± 0.05 °C/min, respectively. In all experiments, to eliminate previous thermal histories, the RD12-filled ECB cell was first heated to isotropic (I) phase and then cooled down to a certain temperature at 1 °C/min. The morphological evolutions of RD12 under a vertically applied electric field were also studied by POM. Here, the electric field with an alternative current (AC) voltage (60 Hz) was applied to the RD12-filled ECB cell using a waveform generator (Tektronix, AFG 3022, USA). Furthermore, utilizing a photodetector (FLUKE, Fluke 196, USA) and a fiber laser

(57) Ryschenkow, G.; Kleman, M. *J. Chem. Phys.* **1976**, *64*, 404.

(UNIPHASE, 1216-2-CE, USA) generating a 635 nm ray, time-dependent transmittance of the RD12-filled ECB cell was monitored with respect to different electric fields.

To confirm the RD12 orientations, which were proposed on the basis of the experimental observations of the RD12-filled ECB cell, we also fabricated in-plane switching (IPS) LC cells.⁵⁸⁻⁶¹ In contrast to the ECB LC cell having planar electrodes both on the top and bottom substrates, the IPS LC cell consists of the interdigitated common and signal electrodes existing only on the bottom substrate. Here, the electrode distance should be kept larger than electrode width and cell gap so that the in-plane field is mainly generated between electrodes. Cell gap (d), electrode width (w), and electrode distance (l) of the RD12-filled IPS cell were controlled to be 4.62, 7.0, and 8.0 μm , respectively.

Results and Discussion

As schematically illustrated in Figure 3a, the RD12-filled electrically controlled birefringence (ECB) cells with planar alignment layers are first fabricated to study molecular orientations of RD12 under vertical electric fields. In the ECB cells, the normalized light transmission can be determined by the following equation^{56-58,62}

$$T/T_0 = \sin^2(2\Psi)\sin^2(\pi d \Delta n_{\text{eff}}(V)/\lambda) \quad (1)$$

where Ψ is the angle between optic axis of LC and crossed polarizers, Δn_{eff} is the voltage-dependent effective birefringence, d is the cell gap, and λ is the wavelength of the incident light. To measure the normalized light transmission in the ECB cells, the optic axis of LC in the initial state (without electric field, 0 V) is arranged to be 45° from the transmission axes of crossed polarizers. Therefore, the cell possesses some transmittance before applying a bias voltage in the ECB cell. On the other hand, when a vertical AC electric field is applied to the ECB cell, the transmittance of the cell can be changed as a result of changing Δn_{eff} . The ECB cell appears to be black if the Δn_{eff} is small enough. Additionally, the transmittance change should be uniform over whole cell area when molecular frustration between LC molecules does not occur in response to applied vertical electric field.

To check the macroscopic RD12 arrangement due to the molecular anchoring forces between RD12 and the planar alignment layers and to verify the reversible electric switching of RD12 by the electric field, we first heated the RD12-filled ECB cell to its I phase and then gradually cooled down to 122.7 °C, which is in the N phase. The POM image taken in the N phase without applying any electric field is shown in Figure 3b. Because the rubbed direction (S) in the initial state is arranged to be 45° from the transmission axes of crossed polarizers, the cell exhibits some transmittance. On the other hand, a complete

dark state is obtained in POM image when it is rotated by 45° (inset of Figure 3b). On the basis of the POM image in Figure 3b, it is obvious that the optic axis of RD12 is macroscopically and uniformly oriented along the S. It is worthy to mention that the whole shape of RD12 is disklike rather than rodlike without alignment layers and electric fields. Therefore, we speculate that the long axis of the rod and the in-plane axis of the disk mesogens in RD12 are aligned parallel to the rubbed direction due to the molecular anchoring forces between RD12 and the planar alignment layers. More detail molecular arrangements with respect to electric field and time will be further discussed later in this paper. When 15 V is applied to the RD12-filled ECB cells, the bright state without a bias voltage (Figure 3b) suddenly switches to a dark state (Figure 3c). This simple POM experiment clearly indicates two facts. One is that both the long axes of the rods and the in-plane axis of the disks of RD12 are well oriented along the rubbed direction. The other is that by applying a vertical electric field the LC director can be reoriented parallel to the electric field, similar to a typical ECB cell with rod-like LCs. Note that orientation of LC director in the RD12-filled ECB cell can be reversibly switched.

Based on the molecular geometry of RD12 as illustrated in Figure 1, we can expect a large birefringence (Δn) of RD12. The Δn of RD12 is estimated at 122.7 °C (in the N phase) by the measurements of retardation ($d\Delta n$) and d of the RD12-filled ECB cell. The optic axis of RD12 is first aligned to one of optic axes of crossed polarizers, and then a quartz retardation plate is inserted between RD12 cell and analyzer. The interference color from RD12 with a quartz retardation plate is observed and compared with the colors in Michel-Lévy birefringence chart which are correlated with retardations. The retardation of RD12 cell is evaluated to be 0.762 μm by rotating the analyzer to the dark state, in which both retardations of the quartz retardation plate and the RD12 cell are identical. This retardation value of RD12 cell also provides an obvious explanation of the greenish color in POM image of the RD12-filled ECB cell without any electric fields (Figure 3b). The estimated retardation of RD12 is also confirmed by utilizing a commercially available optic instrument (Sesim Photonics Technology, REMS-150, Korea). Because d is controlled to be 4.43 μm , Δn of RD12 is calculated to be 0.172 at 122.7 °C. The large Δn of RD12 can be useful for fabricating thin optical compensation films. Furthermore, the birefringence tunability of RD12 by magnetic and/or electric field makes it possible for RD12 to be used as a tunable optical switching material in the electro-optical devices.

To investigate the phase evolutions of the RD12-filled ECB cell, POM textures are monitored during cooling (Figure 4a) and subsequent heating (Figure 4b) at 1.0 °C/min. To remove prehistoric effects of RD12, the RD12-filled ECB cell is first heated to above 145 °C and waited there for 5 min. Upon cooling, the I \leftrightarrow N phase transition occurs at 130 °C (Figure 4a). This is identical with the observation in the RD12 LC cell without any alignment

- (58) Oh-e, M.; Kondo, K. *Jpn. J. Appl. Phys.* **1997**, *36*, 6798.
- (59) Jeon, S. Y.; Shin, S. H.; Jeong, S. J.; Lee, S. H.; Jeong, S. H.; Lee, Y. H.; Choi, H. C.; Kim, K. J. *J. Appl. Phys. Lett.* **2007**, *90*, 121901.
- (60) Jeong, S. J.; Park, K. A.; Jeong, S. H.; Jeong, H. J.; An, K. H.; Nah, C.; Pribat, D.; Lee, S. H.; Lee, Y. H. *Nano Lett.* **2007**, *7*, 2178.
- (61) Oh-e, M.; Yoneya, M.; Kondo, K. *J. Appl. Phys.* **1997**, *82*, 528.
- (62) Hegde, G.; Xu, P.; Pozhidaev, E.; Chigrinov, V.; Kwok, H. S. *Liq. Cryst.* **2008**, *35*, 1137.

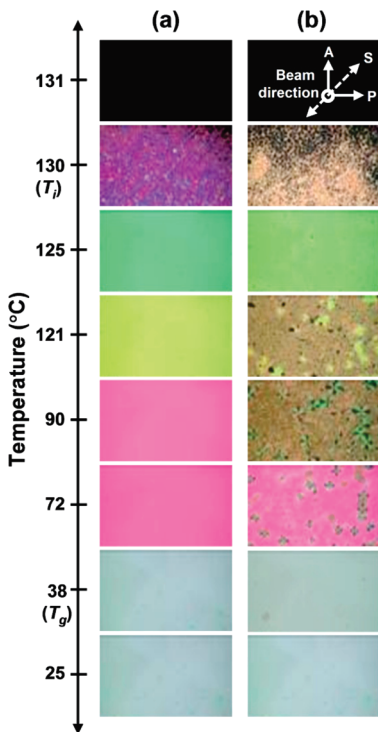


Figure 4. POM images of the RD12-filled ECB LC cell taken at different temperatures during (a) cooling and (b) subsequent heating at 1.0 °C/min.

layers (Figure 2a).⁴⁹ However, the N phase does not transfer to the stable K_{T1} crystalline phase even though the RD12-filled ECB cell is cooled to 25 °C. Note that this temperature is below the glass transition temperature ($T_g = 38$ °C). These experimental observations suggest that molecular anchoring interactions between RD12 and planar alignment layer are strong enough to suppress or delay the crystallization of RD12. In the RD12-filled LC cell without any alignment layers,⁴⁹ a glassy N phase can be obtained by quenching RD12 below T_g (Figure 2b). To support this speculation, we recorded POM textures during the heating process at 1.0 °C/min (Figure 4b). As expected, the glassy N phase is transformed to the metastable K_{T2} phase above T_g . When the temperature reaches to around 90 °C, the metastable K_{T2} phase is transformed to the stable K_{T1} phase. The continuous heating results in the formation of the N phase at 121 °C. More systematic experiments should be carried out to understand the anchoring interactions on the molecular level and to find the origins of the crystallization suppression by the planar alignment layers. Because the main purpose of this research is the investigation of RD12 molecular orientations under vertical electric fields, the rest of experiments are conducted in the N phase, in which RD12 is homogeneously aligned and forms a macroscopic single domain.

Response behaviors of RD12 under vertical electric fields with a frequency of 60 Hz, time-resolved transmittances of the RD12-filled ECB cell are measured with respect to various electric fields. The results are summarized in Figure 5. Upon applying voltage from 0 to 2.5 V, the normalized light transmittance gradually decreases from 7.4 to 1.2 as increasing time from 0 to 1.8 s, and

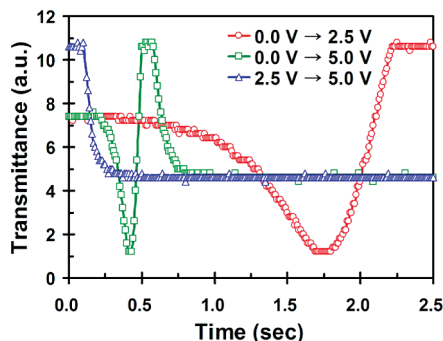


Figure 5. Time-dependent transmittances of the RD12-filled ECB cell with respect to various electrical fields: 0 → 2.5 V, 0 → 5.0 V, and 2.5 → 5.0 V.

rapidly increases, and then levels off to 10.6 when time reaches to 2.22 s, as shown in Figure 5. On the basis of eq 1, the full bright state should be obtained when the phase retardation matches $m + \lambda/2$, where m can be 0, 1, 2, etc. As discussed in Figure 3b, the phase retardation without an electric field is 0.762 μ m. The phase retardation at the initial state is thus slightly smaller than the $3\lambda/2$ phase at 635 nm. Note that RD12 at the initial state is homogeneously aligned parallel to the glass substrates and its optic axis is positioned to be 45° with respect to the crossed polarizers. By applying the voltage from 0 to 2.5 V, RD12 gradually “stands up” toward the vertical electric field, resulting in the decrease of phase retardation. Therefore, the light transmittance decreases to 1.2 when time changes from 0 to 1.8 s, as shown in Figure 5. According to eq 1, the light transmittance of 1.2 indicates that the phase retardation of RD12 in the ECB cell is close to the λ phase, so that the cell shows a dark state. The light transmittance is not 0 even though the phase retardation is the λ phase at 1.8 s because of the wavelength dispersion effect. The optic axis of RD12 is further tilted up toward the vertical electric field when RD12 has a longer relaxation time. Finally, the light transmittance enhances and levels off to be 10.6, of which phase retardation is close to $\lambda/2$. RD12 molecular arrangement under the electric field is stabilized after 2.22 s.

To observe RD12 molecular reorientation behaviors under a high electrical potential difference, we applied a voltage from 0 to 5.0 V. With a higher voltage, RD12 is reoriented from $\sim 3\lambda/2$ phase (at $t = 0$ s) to the λ phase ($t = 0.41$ s), which is 4.5 times faster than the reorientation time when a 2.5 V potential difference is applied (0 V → 2.5 V). Similar to the case of 2.5 V potential difference, however, RD12 is further tilted along the vertical electric field and the full bright state is obtained with the $\lambda/2$ phase at $t = 0.56$ s. After a higher electric field (5.0 V) is applied, RD12 additionally “stands up” and is stabilized to have a retardation much less than the $\lambda/2$ phase. Above $t = 0.93$ s, the light transmittance is 4.6, indicating that the optic axis of RD12 is still not parallel to the beam direction. Therefore, 5.0 V is not strong enough to make a homeotropic molecular alignment of RD12.

The time-dependent transmittances of the RD12-filled ECB cell measured by applying 0 → 2.5 V or 0 → 5.0 V

exhibit similar tendencies, yet the response times to electric field are abnormally slow compared with those of a typical calamitic LC molecule. One of the possibilities of the slow response time could come from the high viscosity of RD12 supermolecules. Another reason could be originated from the molecular frustrations since RD12 is constructed by chemical linkages between the rod and the disk mesogens. This last speculation could be persuasive especially in the antiparallel rubbed ECB cell with planar alignment layers, in which the entire shape of RD12 is ribbonlike rather than the disklike, as discussed in Figure 3. To confirm this speculation, the voltage is first applied from 0 to 2.5 V and waits more than 3.0 s to reach the stabilized state. This stabilization state possesses the maximum bright state, at which the phase retardation is close to the $\lambda/2$ phase. After RD12 stabilization at 2.5 V, the light transmittance is monitored by increasing the applied voltage from 2.5 to 5.0 V, as shown in Figure 5. Upon changing the voltage, the light transmittance rapidly decreases from 10.6 to 4.6 in 0.36 s and is not changed at a longer time. Even though dielectric torque effects according to tilting angles are considered, RD12 under the electric field change from 2.5 to 5.0 V is stabilized six times faster than the electric field change from 0 to 2.5 V. This fast response is partially due to the fact that there is no molecular frustration during the electric field change from 2.5 to 5.0 V. On the basis of the time-dependent transmittances of the RD12-filled ECB cell and the corresponding RD12 molecular arrangements depending on various electric fields, it is provisionally concluded that molecular frustrations occur in a consequence of the competition among the rods attached to both sides of the disk, in which rod-disk molecules are horizontally aligned to form a ribbon-like shape on the antiparallel rubbed substrate in the initial state.

To secure our tentative conclusion and identify more detailed molecular orientations depending on the various electric fields, *in situ* POM textures are recorded under vertical electric fields. Figure 6a represents a series of POM images taken between 0 and 2.22 s under the applied voltage from 0 to 2.5 V. POM images up to 0.36 s are not much changed, which agrees with results of the normalized light transmittance. When time reaches 0.52 s, multidomains with thread textures along the rubbing direction are observed and the greenish (close to the $3\lambda/2$ phase) POM texture at the initial state is changed to bluish (between $3\lambda/2$ and λ phase) and yellowish (between λ and $\lambda/2$ phase) textures. The multidomain POM textures are changed to a homogeneous single domain, when the transmittance is stabilized above 2.22 s. Note that the stabilized state at 2.22 s indicates the bright state (close to $\lambda/2$ phase), as shown in Figure 6a. Based on our best knowledge, a typical rodlike LC molecule does not form the multidomains with thread textures along the rubbing direction in the ECB cell with homogeneous alignment of LC as long as a small pretilt angle is defined. If the multidomain POM textures are originated from a high viscosity of RD12 LC molecule, we may avoid the

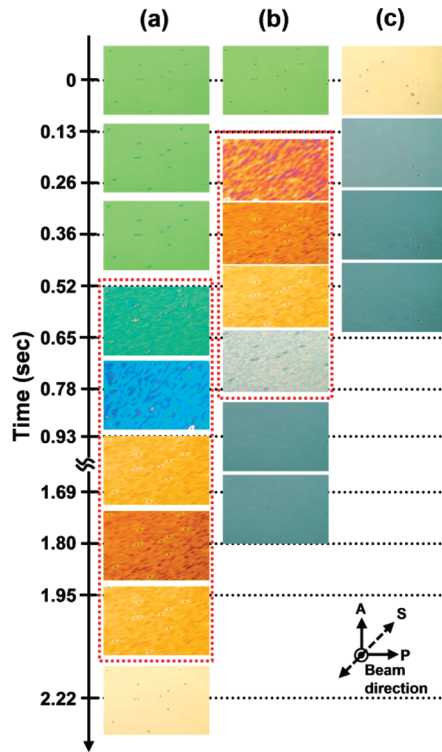


Figure 6. Time-resolved POM images for the RD12-filled ECB cell under vertical electrical fields: (a) $0 \rightarrow 2.5$ V, (b) $0 \rightarrow 5.0$ V, and (c) $2.5 \rightarrow 5.0$ V. POM images of frustrated molecular states were emphasized with red dotted boxes in parts a and b.

formation of the multidomain POM textures by applying a high electrical potential difference. However, the multidomains with thread textures along the rubbing direction are observed even under a high electrical potential difference ($0 \rightarrow 5.0$ V), as shown in Figure 6b. Brightness and color of POM textures are also changed according to the phase retardation. These results are well matched with those of Figure 5. Based on the POM results combined with the normalized transmittance depending on time and electric field, we can conclude that the multidomains with thread textures are formed because of the molecular frustrations under the vertical electric field. Our conclusion is also supported by the POM textures taken under the voltage change from 2.5 to 5.0 V, after the stabilization of RD12 at 2.5 V. The results shown in Figure 6c are also well-matched with those of the normalized light transmittance. As expected, the multidomain texture is not observed and the POM texture is stabilized in 0.36 s that is a reasonable switching time for a viscous LC molecule. This result clearly indicates that RD12 responds with one-step molecular orientation to the vertical electric field without any molecular frustrations after the stabilization at 2.5 V.

By careful analysis of POM textures and light transmittances, we propose the two-step molecular orientations under the vertical electric field. From the POM image of the RD12-filled ECB cell (Figure 3b), it is recognized that the optic axis of RD12 is macroscopically and uniformly oriented along the S without any electric field. The overall shape of RD12 in the ECB cell with the rubbed planar alignment layers must be ribbonlike rather

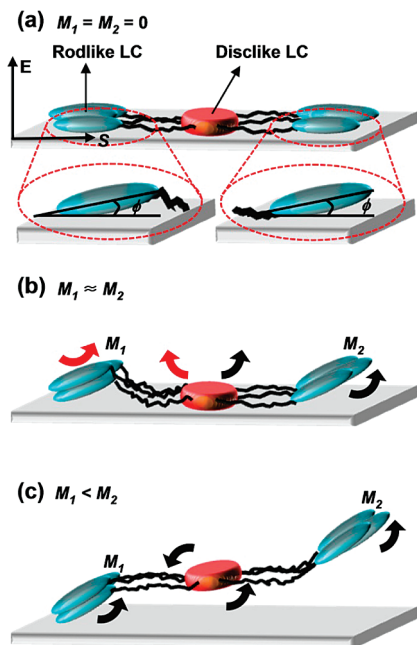


Figure 7. Schematic illustrations of RD12 molecular orientations in the RD12-filled ECB cell: (a) $M_1 = M_2 = 0$, (b) $M_1 \approx M_2$, and (c) $M_1 < M_2$.

than disklike. The most probable molecular orientation without an electric field on the rubbed planar alignment layer is schematically illustrated in Figure 7a. As shown in this figure, the long axes of six rod mesogens chemically attached to the periphery of the disk mesogen are oriented along the rubbed direction with a certain physical pretilt angle (ϕ). The experimentally measured ϕ of RD12 is $\sim 0.80^\circ$. Molecular rearrangement under the vertical AC electric fields can be explained by the dielectric torque (\mathbf{M}) of each mesogen. The dielectric torque, \mathbf{M} , can be expressed with an electric field (\mathbf{E}), a dielectric anisotropy of LC molecule ($\Delta\epsilon$), and a LC director (\mathbf{n}).⁶³

$$\mathbf{M} = |\Delta\epsilon(\mathbf{n}\mathbf{E})\mathbf{n} \times \mathbf{E}| \quad (2)$$

Before discussing the molecular orientation under the AC electric fields, it is worthy to point out that the triphenyl disk mesogen does not respond to the DC electric field below 150 V.⁵⁰ Therefore, by applying AC electric field from 0 to 5 V, the triphenyl disk mesogen does not play as an active mesogen to rearrange RD12, yet works as a chemical junction point holding six mesogens. When a vertical electric field from 0 to 5 V is applied, two dielectric torques, \mathbf{M}_1 and \mathbf{M}_2 , exert on the left and right parts of the rod mesogens attached to the disk mesogen, respectively (Figure 7b). In the first step, \mathbf{M}_1 and \mathbf{M}_2 compete with each other to align toward the electric field, whereas the disk mesogen behaves like an anchor of RD12. As illustrated in Figure 7b, \mathbf{M}_2 has a favoring position to win this competition compared with \mathbf{M}_1 because rods of \mathbf{M}_2 can easily “stand up” with less resistance than rods of \mathbf{M}_1 . When the competition among the rod mesogens is over, \mathbf{M}_2 becomes a dominant driving

(63) Gu, M.; Shlyanovskii, S. V.; Lavrentovich, O. D. *Phys. Rev. Lett.* 2008, 100, 237801.

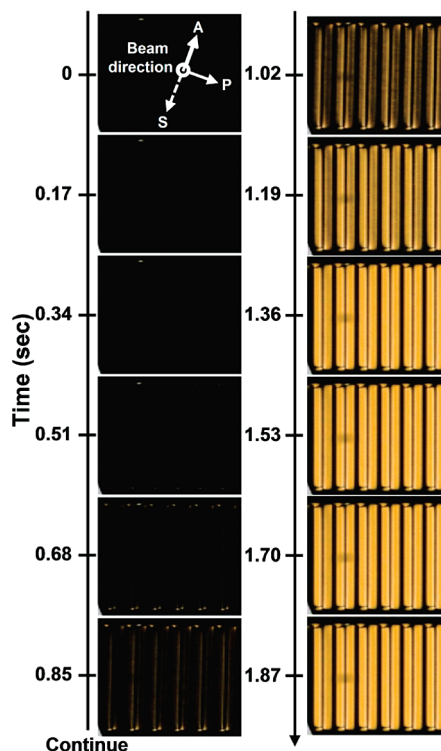


Figure 8. Time-resolved POM images for the RD12-filled IPS cell under an in-plane electric field from 0 to 5.0 V.

force to control the alignment of the whole RD12 molecule, as shown in Figure 7c. After the molecular competitions between \mathbf{M}_1 and \mathbf{M}_2 , the in-plane axis of the disk mesogen also gradually tilt up to the electric field due to the alignment of rod mesogens. Therefore, it is evident that the peculiar molecular frustration of RD12 under a vertical AC electric field is originated from the chemical attachment between the rod and the disk mesogens.

To confirm the molecular frustration and rearrangement of RD12 under the AC electric field, the RD12-filled in-plane switching (IPS) LC cell is also fabricated. In the IPS cell, the optic axis of LC should rotate along the in-plane direction unlike in the ECB cell and the transmittance change follows eq 1. Its POM images under the AC electric field in a range from 0 to 5.0 V are monitored with respect to time, as shown in Figure 8. Because the rubbing direction is parallel to analyzer ($\Psi = 0^\circ$), the POM image of the RD12-filled IPS LC cell appears dark without a bias voltage. This result confirms the fact that the long axes of the rods and the in-plane axes of discs of RD12 are uniformly aligned parallel to the rubbed direction which is about 20° clockwise rotated with respect to electrode directions. The molecular arrangement of RD12 in the IPS LC cell without an electric field is schematically illustrated in Figure 9. By applying the in-plane AC electric field from 0 to 5 V, the multidomains with thread textures that are formed because of the molecular frustrations in the RD12-filled ECB cell are not generated in the RD12-filled IPS cell. Only one-step transition is observed as shown in Figure 8. On the basis of the POM experimental results, RD12 molecular orientations in the RD12-filled IPS LC cell are proposed and

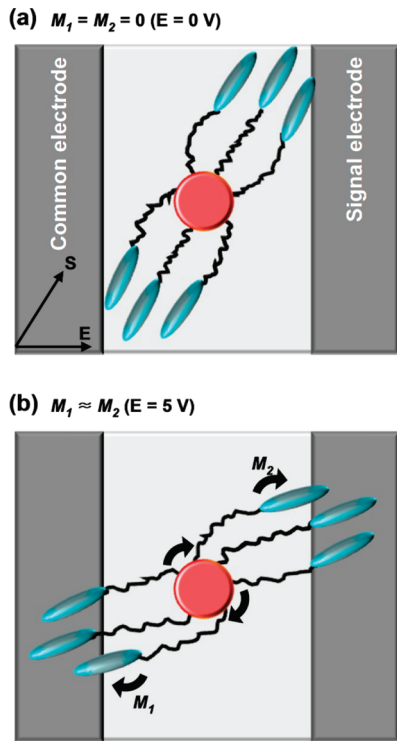


Figure 9. Schematic illustrations of RD12 molecular orientations in the RD12-filled IPS cell: (a) $E = 0$ V and (b) $E = 5.0$ V.

schematically illustrated in Figure 9a and 9b. When the in-plane AC electric field is applied to the RD12-field IPS LC cell, the rod mesogens, pointing to either northeast or southwest, rotate clockwise toward the electric field without any molecular competitions and frustrations, as shown in Figure 9b. RD12 molecular orientation under the in-plane electric field is also supported by the measurement of light transmittance. Therefore, we can

confirm our conclusion that the molecular frustration in the RD12-filled ECB cell is originated from the competitions between the rod mesogens attached on both sides of the disk mesogen (Figure 7b).

Conclusions

Molecular orientation of a rod-disk LC molecule (RD12) under various AC electric fields is investigated in the vertical and in-plane electric field LC cells. Possible molecular orientations are proposed on the basis of the POM images combined with the normalized transmittance light. In the vertical electric field LC cell, RD12 responds to the electric field with a two-step process. On the basis of our experimental observations and analyses, it is recognized that the molecular frustrations forming multidomains with thread textures occur as a result of the competition between the rod mesogens attached to both sides of the disk mesogen. After the frustration and stabilization of the rod mesogens, the whole RD12 molecule is aligned parallel to the electric field. This peculiar two-step molecular orientation of RD12 should be attributed to the chemical attachment between the rod and the disk mesogens and the specific geometry of the vertical electric field LC cell. This conclusion is further confirmed in the in-plane electric field LC cell, which consists of the interdigitated common and signal electrodes. The unique molecular behaviors of RD12 under the AC electric fields can be applied in electronics, optics, and energy.

Acknowledgment. This research was supported by WCU (R31-2008-000-20029-0) and Basic Science Research (NRF-2010-0007562) programs funded by the Korean government (MEST). The part of the work at University of Akron was supported by NSF (DMR-0516602 and DMR-0906898).